

Fault-tolerant control of a permanent magnet synchronous motor based on hybrid control strategies using a multi-variable filter

Miloud Bahiddine^{1,2}, Ali Belhamra²

¹Department of Electrical Engineering, Faculty of Technology, University of Mohamed Boudiaf, M'sila, Algeria

²Laboratory Systems Electromechanical, Department of Electromechanical, Faculty of Technology, University Badji Mokhtar, Annaba, Algeria

Article Info

Article history:

Received May 24, 2023

Revised Oct 28, 2023

Accepted Dec 30, 2023

Keywords:

Direct torque control

Fault tolerant control

Multi-variable filter

Sliding mode control

Space vector modulation

Torque ripples

Two-level voltage inverter

ABSTRACT

This paper describes direct torque control (DTC) of a permanent magnet synchronous machine (PMSM) powered by a two-level voltage inverter whose switching of switches is based on the space vector modulation (SVM). To enhance the robustness of control in the presence of faults, we have enhanced DTC with SVM by incorporating a multivariable filter to address fault current effects. In this modification, traditional proportional-integral controllers are substituted with sliding mode controllers. This approach results in a revised structure known as DTC-SVM with sliding mode control, presenting a new fault-tolerant control diagram. A comparative study between these different control strategies is carried out. The simulation results show clearly the interest of a multi-variable filter association with the DTC-SVM-sliding mode control² (SMC²) in degraded mode. The outcomes achieved provide substantial evidence supporting the resilience and efficacy of this approach, especially when confronted with the influence of the faults current.

This is an open access article under the [CC BY-SA](https://creativecommons.org/licenses/by-sa/4.0/) license.



Corresponding Author:

Miloud Bahiddine

Department of Electrical Engineering, Faculty of technology, University of Mohamed Boudiaf

M'sila, Algeria

Email: miloud.bahiddine@univ-msila.dz

1. INTRODUCTION

The fault-tolerant control for permanent magnet machines is crucial to ensure their reliable operation even in the presence of potential faults or failures. Permanent magnet machines find application in diverse fields such as electric vehicles, renewable energy systems, and industrial automation. Their usage spans a range of sectors, showcasing their versatility and adaptability to different technological contexts, and ensuring their continuous operation is essential for the overall system reliability [1]. Fault-tolerant control strategies aim to detect faults, isolate the affected components, and enable the system to continue functioning with minimal performance degradation [2]. The fault-tolerant control strategies can be crucial for ensuring the reliable operation of permanent magnet machines, particularly in the presence of faults or other disturbances. Additionally, mitigating torque ripple is important to improve the overall performance and efficiency of these machines [3]. Here are some sources of torque ripple. Nonlinearities in the inverter and control system, such as switching delays or inaccuracies in the current control loop, can introduce disturbances that result in torque ripple [4]. Another source of torque ripple is related to the harmonics of the electromotive force (torque ripple) [5]. Their amplitude is proportional to the value of the current and depends on the spatial distribution of the magnetic field in the gap. From this expression, we can note that the

torque only has multiple rank harmonics of six [6]; the harmonics of torque are proportional to the amplitude of the current. The fem multiple ranks of three do not produce torque ripples [5]. An unbalance of the phase currents in case of a fault induces changes in the direct and quadrature components of the stator current leads to the generation of low frequency torque harmonics (twice the supply frequency) [7]. This harmonic is proportional to the product of the fundamental of the electromotive force and the amplitude of the current [5], [8]. The consequences of torque ripples are numerous: vibrations in rotating machines, audible noise, risk of excitation of mechanical eigen modes, inaccuracies of movement control; they can cause destruction of the material [9]. Reducing torque ripples can be handled in two ways: i) method consists of modifying the shape of the supply currents by adding current harmonics related to the torque ripples (modify the motor structure) [10], and ii) using multi-variable filter (MVF) is designed to reduce undesirable harmonics in the AC power supply that could affect the motor's torque and flux [11]. Harmonics can cause fluctuations in the current and voltage, which in turn can lead to torque and flux variations. By mitigating harmonics, the filter helps maintain stable torque and magnetic flux levels [12].

The objective of this work is to study, develop a fault-tolerant control strategy for a permanent magnet synchronous machine (PMSM). The fault tolerant in control techniques such as direct torque control (DTC)-space vector modulation (SVM)-sliding mode control (SMC) can achieved by implementing specific strategies in the control of electric motors [13]. Here are some of the commonly used methods to ensure some fault tolerance in these control techniques: i) sensor redundancy: the use of multiple sensors can enable rapid detection and correction of possible faults, thus ensuring continuity in control even in the presence of failures, ii) on-board diagnostics: the integration of advanced diagnostic systems can enable early detection of potential faults, making it easier to take corrective and preventive measures to ensure uninterrupted engine operation [14], iii) adaptive control: implementing adaptive control strategies allows the system to automatically adjust in the event of a fault, thereby ensuring continuity of control and reducing the negative effects of faults on motor performance, and iv) repair control: the use of repair control techniques allows faults to be bypassed or corrected in real time, thereby maintaining stable and efficient engine operation even in the presence of faults [15].

By integrating these fault tolerance strategies into DTC-SVM-SMC control techniques, it is possible to ensure continuous and reliable operation of the electric motor, even in the presence of faults or adverse conditions [13]–[16]. This helps improve the durability and dependability of control systems, which are crucial in many critical industrial applications [17]. To overcome the robustness of the control strategies into DTC-SVM-SMC in the presence of a fault effect, we included an improvement of the DTC with SVM by the use of a multivariable filter for the fault current effect, where the presence of the continuous component in stator current [16]–[18]. This control method allows giving a new structure DTC-SVM-SMC with a MVF (new fault-tolerant control diagram) [19].

The principle of the MVF in the command strategies of DTC-SVM and SMC is to improve the efficiency and precision of these advanced control techniques used in electric motor control systems [19]–[20]. Multivariable filters are utilized to optimize the overall system response and stability, particularly in terms of torque and flux control [21]. Implement a MVF that can detect anomalies or deviations in multiple system variables (fault detection and isolation). This filter should be designed to distinguish between normal variations and faults, providing accurate fault diagnosis and isolation. To fulfill the primary aim outlined in the research [22], this article contributes by implementing a fault-tolerant hybrid control using the DTC-SVM-SMC technique, incorporating a MVF [23]–[24]. A comparative analysis was conducted between the proposed DTC-SVM-SMC2-MVF method and the DTC-SVM-SMC control without MVF, specifically under the conditions of a stator current fault (the presence of the continuous component in stator current) [24].

This article is structured into several sections; the PMSM mathematical representation is outlined in section 3. In section 4 the estimation of stator flux is presented. Section 5 explains the DTC-SVM-SMC method. Section 6 explains the new fault tolerant control strategy. In section 7 you will find the outcomes of the simulation, which substantiate the strength and robustness of the suggested method under various operating conditions. in the section 8 healthy case (pre-fault). Section 9 degraded mode (post- fault) without MVF and in section 10 fault-tolerant control based on hybrid control strategies, DTC-SVM with second order SMC using MVF. The section 11 explains the comparative study between the different mode conditions. The finally section concludes this paper.

2. SECOND ORDER SLIDING-MODE CONTROL DESIGN

The second-order SMC is a nonlinear control method rule may by effective to remove the chattering phenomenon [16]–[24]. The system's drive is modified through the application of a discontinuous control signal, which compels the system to move in a predetermined sliding mode. In view of that, the global scheme for the PMSM with detailed control algorithms is given in Figure 1.

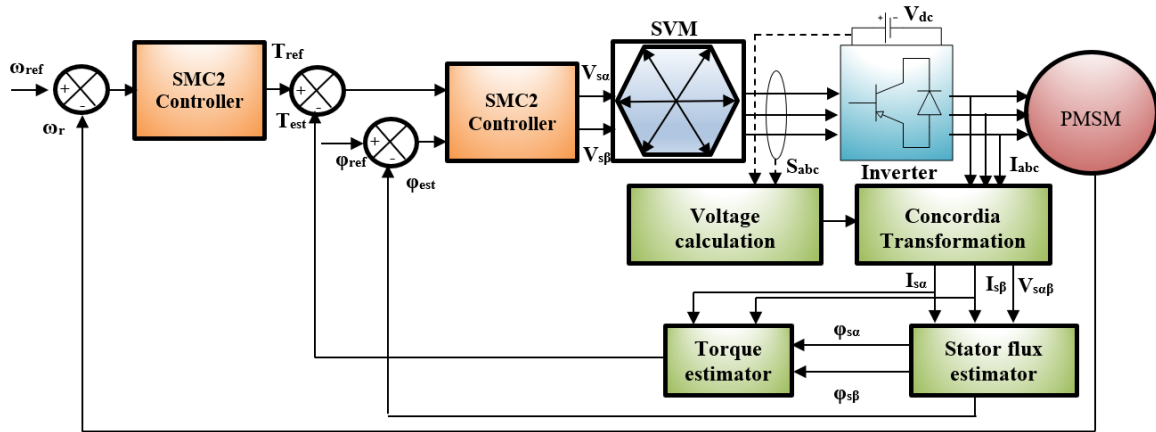


Figure 1. Block diagram of DTC-SVM with second order SMC for PMSM drives

2.1. Permanent magnet synchronous motor model

The electrical equations of the PMSM, when formulated in the park reference frame are represented by:

$$\frac{d}{dt} i_d = \frac{-R_s}{L_d} i_d + \frac{\Omega L_q}{L_d} i_q + \frac{V_d}{L_d} \tag{1}$$

$$\frac{d}{dt} i_q = \frac{-R_s}{L_q} i_q - \frac{\Omega L_d}{L_q} i_d - \frac{\Omega \psi_f}{L_q} + \frac{V_q}{L_q} \tag{2}$$

$$J \frac{d}{dt} \Omega = (\Gamma_e - \Gamma_L - f \Omega) \tag{3}$$

$$\frac{d}{dt} \theta_e = \omega_e \tag{4}$$

$$\Gamma_e = p \Phi_f i_q + p(L_d - L_q) i_d i_q \tag{5}$$

Where the electrical parameters are: i_d and i_q are the dq axis stator currents, ω_e is the electrical angular velocity, θ_e is the rotor position V_d and V_q are the d and q axis stator voltages, R_s is the stator per-phase resistance, L_d and L_q are the dq axis stator inductances.

The mechanical parameters are: p is the number of the pole pairs, Ψ_f is the magnet's flux linkage, Γ_e and Γ_L are respectively the electromagnetic and the load torques, F is the frictional coefficient and J is the moment of inertia. As outlined in the introduction, the fluctuating torque observed in the PMSM is attributed to diverse factors, including the cogging torque effect, uncertainties in design and discrepancies in stator current or imbalances in stator phases. Consequently, the electromagnetic torque can be represented as the combination of the main DC component and harmonic components [10].

$$\Gamma_e = \Gamma_{e0} + \Gamma_{eh} \tag{6}$$

For example, the imprecision of sensors is associated with inherent DC offsets originating from the process of converting signals from the controller's input and the phase current probe [17]. The occurrence of a DC offset in stator current measurements induces oscillations in pulsating torque at the fundamental frequency and can be represented as such.

$$\Delta \Gamma_{e,1} = K_t \cos(\theta_e + \alpha) \sqrt{\Delta i_{as}^2 + \Delta i_{as} \Delta i_{bs} + \Delta i_{bs}^2} \tag{7}$$

For conditioning problems, the current scaling error which arises from analog to digital then from digital to analog forms causes torque oscillation at twice the fundamental frequency can be described as (8) [7]–[8]:

$$\Delta \Gamma_{e,2} = K_{t1} K_t \frac{1}{\sqrt{3}} (\cos(2\theta_e + \frac{\pi}{3}) + 0.5) \tag{8}$$

2.2. Estimation of stator flux

The components of the stator flux can be represented by utilizing stator resistance, stator voltages, and currents in the fixed reference (α , β) [25]–[26]. Typically, the stator flux is estimated by (9):

$$\begin{aligned}\Phi_{s\alpha} &= \int_0^t (V_{s\alpha} - R_s \cdot I_{s\alpha}) dt \\ \Phi_{s\beta} &= \int_0^t (V_{s\beta} - R_s \cdot I_{s\beta}) dt\end{aligned}\quad (9)$$

The stator flux magnitude can be calculated as (10):

$$\Phi_s = \sqrt{\Phi_{s\alpha}^2 + \Phi_{s\beta}^2}\quad (10)$$

The stator flux angle can be calculated as (11):

$$\theta_s = \arctg \frac{\Phi_{s\beta}}{\Phi_{s\alpha}}\quad (11)$$

The components of the stator voltage ($V_{s\alpha}$, $V_{s\beta}$) are determined through the application of the Concordia's transition to the output voltage of the voltage source inverter (VSI).

$$\begin{bmatrix} V_{s\alpha} \\ V_{s\beta} \end{bmatrix} = \sqrt{2/3} \begin{bmatrix} 1 & -1/2 & -1/2 \\ 0 & \sqrt{3}/2 & -\sqrt{3}/2 \end{bmatrix} \begin{bmatrix} V_{sa} \\ V_{sb} \\ V_{sc} \end{bmatrix}\quad (12)$$

The output voltages of the VSI are given in (13):

$$\begin{aligned}V_{sa} &= \frac{V_{dc}}{3} (2S_a - S_b - S_c) \\ V_{sb} &= \frac{V_{dc}}{3} (S_b - 2S_c - S_a) \\ V_{sc} &= \frac{V_{dc}}{3} (S_c - S_a - 2S_b)\end{aligned}\quad (13)$$

The stator currents' components ($I_{s\alpha}$, $I_{s\beta}$) are determined through the application of the concordia transformation to the measured currents [9]:

$$I_{s\alpha} = \sqrt{2/3} [I_{sa}]\quad (14)$$

$$I_{s\beta} = \frac{1}{\sqrt{2}} [I_{sb} - I_{sc}]\quad (15)$$

2.3. Control strategy

The objective of this section is to develop a PMSM controller utilizing the twisting controller technique. Following the conventional method employed in the control of non-salient PMSM, the direct current reference i_d^{ref} is set to zero, and the quadratic current component i_q^{ref} is directly determined from the outer loop of the speed control [8]. Subsequently, the input controls for the dq-axes are computed using a decoupling control method based on the twisting controller type. The convergence condition is defined by the equation of Lyapunov.

$$\zeta_{m1} \dot{\zeta}_{m1} < 0\quad (16)$$

To assure current convergence to their references, a second-order sliding mode strategy is used. Consequently, sliding mode surface is selected as:

$$\begin{cases} \zeta_{m1} = \dot{\Phi}_s^* - \Phi_s \\ \zeta_{m2} = \dot{\Gamma}_e^* - \Gamma_e \end{cases}\quad (17)$$

Derivative of sliding mode surface:

$$\begin{cases} \dot{\zeta}_{m1} = (V_{sd} - R_s i_{sd} + L_s p \Omega_t i_{sq}) + \Phi_f - \Phi_s^* \\ \dot{\zeta}_{m2} = p \Phi_f \left(\frac{1}{L_s} (V_{sq} - R_s i_{sq} - L_s p \Omega_t i_{sd} - K_A p \Omega_t) \right) - \dot{\Gamma}_e^* \end{cases} \quad (18)$$

If we define the function G1 and G2 as (19):

$$\begin{cases} G_{m1} = (-R_s i_{sd} + L_s p \Omega_t i_{sq}) + \Phi_f - \Phi_s^* \\ G_{m2} = p \Phi_f \left(\frac{1}{L_s} (-R_s i_{sq} - L_s p \Omega_t i_{sd} - K_A p \Omega_t) \right) - \dot{\Gamma}_e^* \end{cases} \quad (19)$$

When the derivative of the sliding mode surface first includes the control input, the system's relative degree becomes one. This fulfills the prerequisite for the relative degree in second order SMC. Consequently, the application of the super-twisting algorithm is implemented [17].

$$\begin{aligned} V_{sd} &= V_{sd1} - \lambda_{m1} \cdot |\sigma_{m1}|^{0.5} \cdot \text{sign}(\sigma_{m1}) \\ \dot{V}_{sd1} &= -\alpha_{m1} \cdot \text{sign}(\sigma_{m1}) \\ V_{sq} &= V_{sq1} - \lambda_{m2} \cdot |\sigma_{m2}|^{0.5} \cdot \text{sign}(\sigma_{m2}) \\ \dot{V}_{sq1} &= -\alpha_{m2} \cdot \text{sign}(\sigma_{m2}) \end{aligned} \quad (20)$$

where the constants α_{m1} , α_{m2} , λ_{m1} and λ_{m2} so that:

$$\begin{cases} \alpha_{m1} > L_s \Phi_{m1}, \lambda_{m1}^2 \geq \frac{4\Phi_{m1} \Gamma_{mM1} (\alpha_{m1} + \Phi_{m1})}{\Gamma_{mM1}^2 \Gamma_{mM1} (\alpha_{m1} - \Phi_{m1})} \\ \alpha_{m2} > L_s \Phi_{m2}, \lambda_{m2}^2 \geq \frac{4\Phi_{m2} \Gamma_{mM2} (\alpha_{m2} + \Phi_{m2})}{\Gamma_{mM2}^2 \Gamma_{mM2} (\alpha_{m2} - \Phi_{m2})} \end{cases} \quad (21)$$

3. A NEW STRATEGY FOR FAULT-TOLERANT CONTROL

The development of the fault-tolerant control presented here relies on the block for fault detection and compensation (FDCB). In this study, the removal of fault terms in control voltage components is achieved by directly extracting the fundamental components in the (α, β) axes. Applying this theory to a faulty case controlled by BSC yields as follows:

$$v_{s\alpha\beta 1}(t) = e^{j\omega t} \int e^{-j\omega t} \hat{v}_{s\alpha\beta 1}(t) dt \quad (22)$$

$$v_{s\alpha\beta 2}(t) = e^{j\omega t} \int e^{-j\omega t} \hat{v}_{s\alpha\beta 2}(t) dt \quad (23)$$

After using the Laplace transformation, the expression for (24) can be represented by the subsequent transfer function:

$$H(s) = \frac{v_{s\alpha\beta 1}}{\hat{v}_{s\alpha\beta 1}} = \frac{S + j\omega_F}{S^2 + (\omega_F)^2} \quad (24)$$

Presently, let's perform a graphical analysis of the system according to (26). By introducing two constants denoted as in (25), the updated transfer function is formulated as (25):

$$H(s) = K_2 \frac{(S + K_1) + j\omega_F}{(S + K_1)^2 + (\omega_F)^2} \quad (25)$$

By putting $K_2 = 20$ and varying, the alignment of input signals and their fundamental frequencies is characterized by a phase relationship with $f = 50$ Hz because $\text{Arg}|H(s)| = 0$ rd. On the flip side, it is evident from the Bode magnitude that the Mag $|H(s)| = 0$ dB at $K_1 = 20$, therefore, $K_1 = K_2 = K = 20$. The novel representation of $H(s)$ in this instance is provided as in (26):

$$H(s) = K \frac{(S + K) + j\omega_F}{(S + K)^2 + (\omega_F)^2} \quad (26)$$

From (27), the components of the control voltages and their fundamentals have the following relationship:

$$\begin{cases} \hat{v}_{s\alpha 1}(s) = \frac{K}{s} [v_{s\alpha 1}(s) - \hat{v}_{s\alpha 1}(s)] - \frac{\omega_F}{s} \hat{v}_{s\beta 1}(s) \\ \hat{v}_{s\beta 1}(s) = \frac{K}{s} [v_{s\beta 1}(s) - \hat{v}_{s\beta 1}(s)] - \frac{\omega_F}{s} \hat{v}_{s\alpha 1}(s) \end{cases} \quad (27)$$

Where K and G are the adjusting constants, $V_{s\alpha 1}$ and $V_{s\beta 1}$ are the components of the control voltages in the stationary reference (α, β) and ω_F is the fundamental pulsation. In view of that, the global scheme for the PMSM with detailed control algorithms is given in Figure 2.

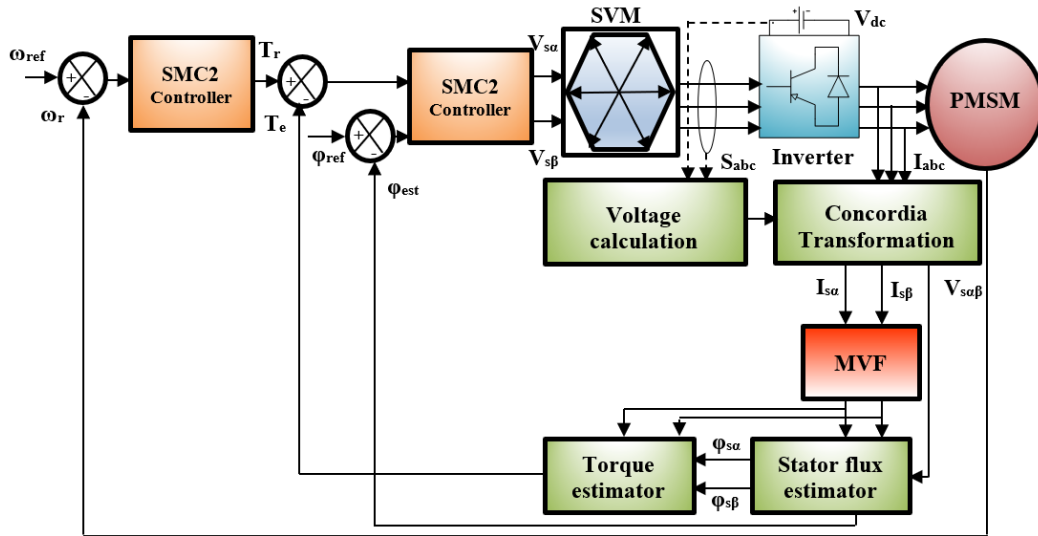


Figure 2. The diagram of the fault- tolerant control strategy for PMSM drives

4. SIMULATION RESULTS AND INTERPRETATION

The control strategy DTC-SVM-SMC2, which was previously introduced, was executed using MATLAB/Simulink software. The subsequent section will showcase both the simulation process and the outcomes yielded by this control approach. The simulation's motor parameters are listed in Table 1.

Table 1. Simulation's motor parameters

Parameters	Rated values
Power rating	1.5 kw
Stator voltage	230/380 V
Frequency	50 Hz
Stator resistance	1.4 Ω
D-axis inductance	0.0066 H
Q-axis inductance	0.0058 H
Rated flux	0.30 Wb
Number of pole pairs	p = 3
Viscous Friction coefficient	0.003881 Nm.s/rad
Permanent magnet flux linkage	0.1546 Wb
Moment of inertia	0.176 ²

4.1. Healthy case (pre-fault)

During this simulation, various tests are conducted within the MATLAB/Simulink environment to demonstrate the effectiveness of the sec control in both transitional and permanent operating conditions for a balanced PMSM. The Figure 3 shows the speed rotor, estimated torque, stator current, stator flux magnitude and the circular trajectory with DTC-SVM-SMC2 scheme. Figure 3(a) show the speed response; the speed continues its reference without static error. The disturbance rejection at the speed level is fast. Figure 3(b)

shows the torque response for a PMSM drive controlled by the DTC-SVM-SMC2 strategy. At the beginning, the motor operates without any load torque, and the electromagnetic torque within the machine progressively aligns with the subsequently applied load torque, exhibiting a few oscillations during the startup phase. At $t=0.2$ s, a load torque of 14 Nm is introduced, causing the electromagnetic torque to undergo oscillations, reaching its peak value before stabilizing at $t=0.25$ s.

Figure 3(c) shows that the flux to a good dynamic and static response with a transient regime a little faster, it follows suitably reference that which is shown in Figure 3(d) where the evolution of the stator flux is circular. Reducing torque and flux fluctuations leads to a decrease in harmonics (good switching of the switches) and consequently fewer problems for the motor (heating, vibration, aging...). The DTC-SVM-SMC2 technique has good dynamic performance and robustness.

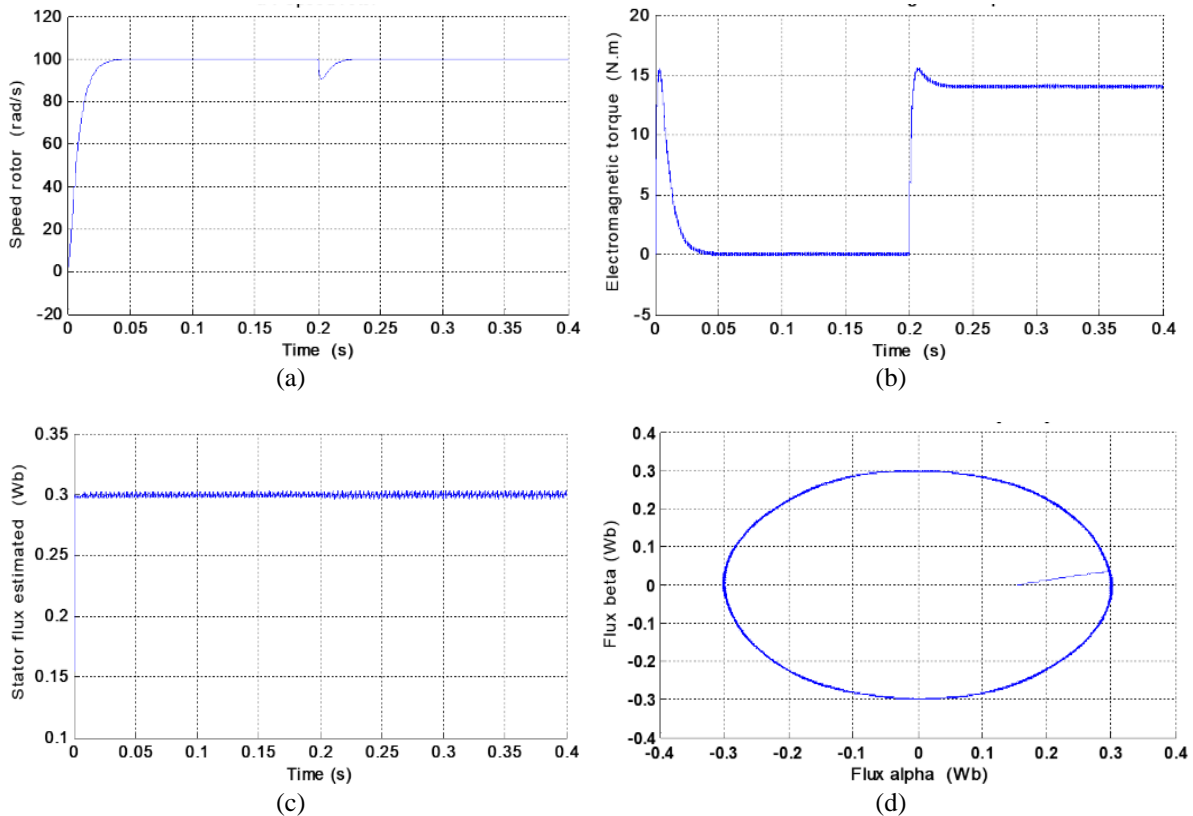


Figure 3. Simulation with a healthy model in load $T_r=14$ N.m: (a) speed rotor, (b) electromagnetic torque, (c) stator flux estimator, and (d) stator flux circular trajectory

4.2. Degraded mode (post- fault) without multi-variable filter

The Figure 4 shows the speed rotor, estimated torque, stator flux and stator current with DTC-SVM-SMC2 scheme in the presence of fault. We conducted a simulation of the system's drive in a degraded mode at a reference speed of 100 (rd/s) load at startup. At $t=0.2$ s, The PMSM follows a load torque equal to 14 Nm. The Figure 4 shows the responses results for DTC-SVM-SMC2 without a multivariabe filter. We note that when the motor starts, the rotor speed Figure 4(a) does not follow its reference speed and exhibits large fluctuations, the value of the ripple and the overshoots in rotor speed is higher than the healthy case, Figure 4(b) illustrates the evolution of the electromagnetic torque in the fault case of an imbalance of phase currents. Then the torque has large variations and is more difficult to match their reference, the ripple and oscillation phenomenon observed on the progression of the electromagnetic torque, Figure 4(c) illustrates the establishment of the stator flux has strong sawtooth ripples, and Figure 4(d) shows the stator flux's evolution in the two-phase reference (α , β), leaves its circular shape and becomes a hexagonal curve, which causes a large deformation in the stator current.

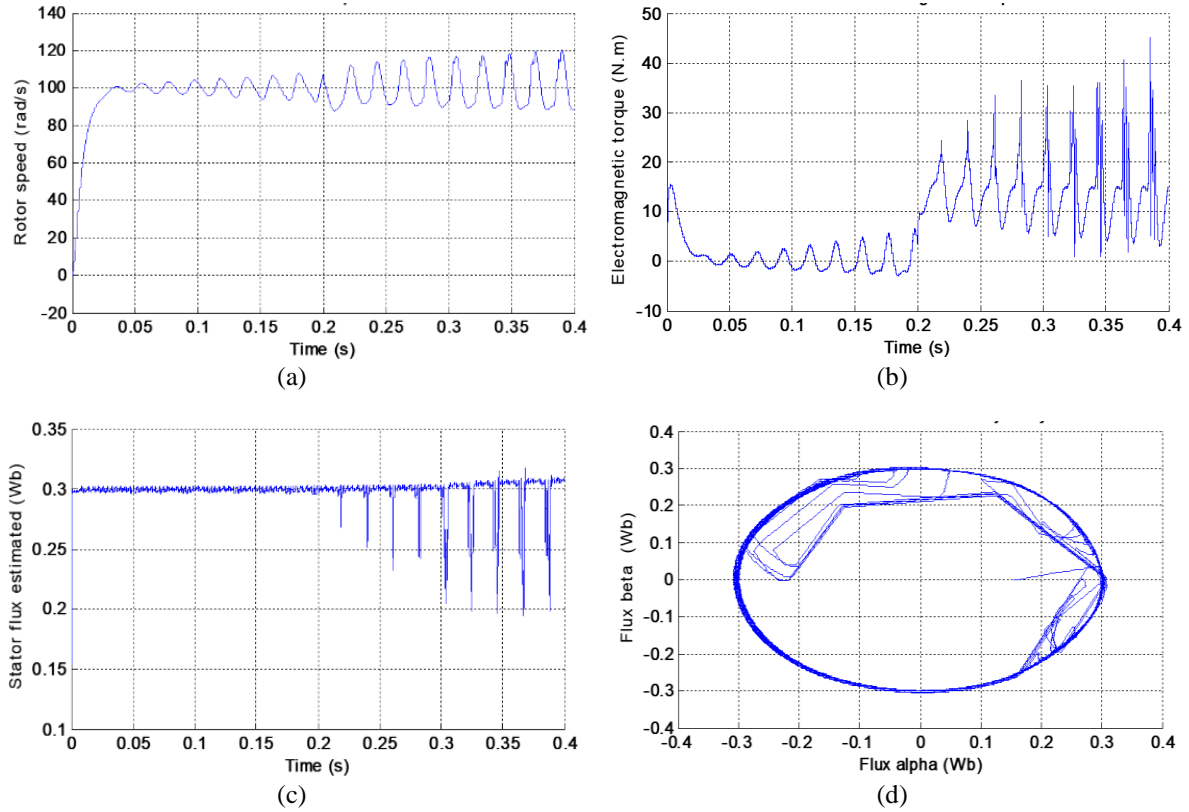


Figure 4. Simulation results with a degraded mode and presence of fault in load $T_r=14$ N.m: (a) speed rotor, (b) electromagnetic torque, (c) stator flux circular trajectory, and (d) stator flux estimator

5. FAULT TOLERANT CONTROL BASED ON HYBRID CONTROL STRATEGIES DTC-SVM WITH SECOND ORDER SLIDING MODE CONTROL USING A MULTI-VARIABLE FILTER

This new fault-tolerant control diagram proposed of DTC-SVM-SMC2 with MVF. MVF is applied to a PMSM, which enables the reduction of the current stator ripple. The Figure 5 shows the speed rotor, estimated torque, stator current, stator flux magnitude and the circular trajectory with DTC-SVM-SMC2-MVF scheme in the presence of fault. Compared to the waveform of the current, the traditional model without a MVF maintains the Sine waveform, but there is a small pulsation, there are harmonics that will lead to a torque ripple in the waveform; while the current.

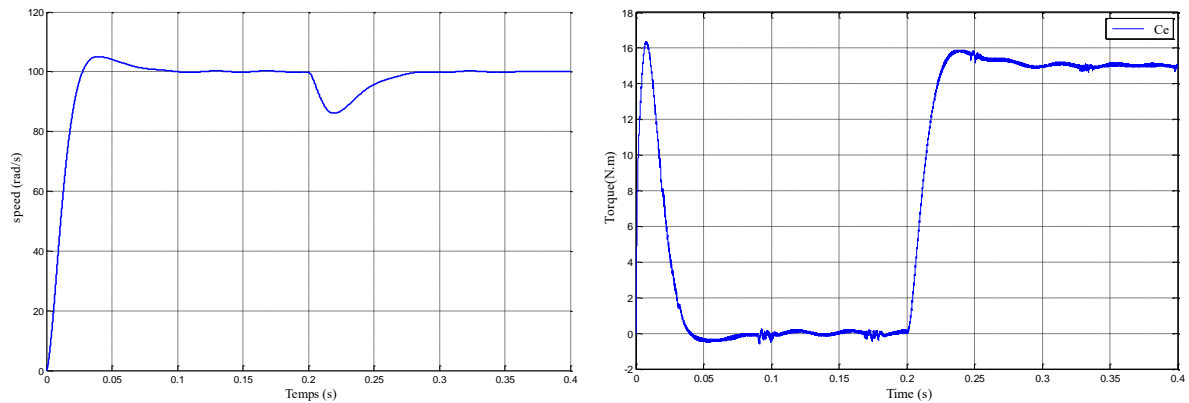


Figure 5. Simulation results of DTC-SVM-SMC2-MVF with a fault (rotor speed and electromagnetic torque)

The waveforms of the DTC-SVM-SMC2 control with MVF and in the presence of a fault are relatively smooth, therefore effectively reduces the harmonic, and the speed continues its reference without static error, the disturbance rejection at the speed level is fast. Fluctuations in torque and flux are reduced mainly in the DTC-SVM-SMC2 with MVF, which results in a reduction of harmonics and consequently fewer problems for motor drives. The DTC-SVM-SMC2 control associated with the MVF has good performance compared to the control without MVF less fluctuations in the torque; the application of MVF leads to a reduction in torque ripples and improves the dynamics and stability of the system.

6. COMPARATIVE STUDY BETWEEN THE DIFFERENT MODE CONDITIONS

A comparative study between these different control strategies is carried out. The simulation results show clearly the interest of a MVF association with the DTC-SVM-SMC2 in degraded mode. In this context, we outline three widely recognized performance criteria commonly employed in assessments. These criteria involve considerations of the error: the squared error's integral (ISE), the integral of the error's absolute value multiplied by time (ITAE), and the integral of the error's absolute value (IAE). They are defined respectively as follows. The IAE:

$$IAE = \int_0^t |e(t)| \cdot dt$$

The ISE:

$$ISE = \int_0^t e^2(t) \cdot dt$$

The ITAE:

$$ITAE = \int_0^t t \cdot |e(t)| \cdot dt$$

The efficiency of the DTC-SVM-SMC2 method, incorporating the multivariable filter, was validated through a comparative analysis employing the three performance criteria includes IAE, ISE, and ITAE [26]. Table 2 showcases the diminished values obtained for each criterion. We note that for the DTC-SVM-SMC2 method with the multivariable filter, the ISE, IAE and ITAE criteria take low values in degraded mode it is almost equals in the healthy case.

Table 2. The values of performance indexes

Mode conditions	Healthy case (pre-fault)	Degraded mode (post- fault) without MVF	Fault mode (post-fault) with MVF
Speed	ISE	53.1	67.3
	IAE	1.007	2.743
	ITAE	0.02932	0.5111
Torque	ISE	0.003151	0.0667
	IAE	0.0302	0.04785
	ITAE	0.006012	0.01252

7. CONCLUSION

The results obtained affirm the validity of the method, robustness and effectiveness and show that regulation with the MVF in the presence of a fault shows good performance in terms of monitoring and rejecting disturbances. This comparison shows clearly that the DTC-SVM-SMC2 method with the multivariable filter gives good performance, and it is robust when the fault current effect is present. This work's goal is to develop and implement a fault-tolerant control strategy based on DTC-SVM with a second-order SMC and MVF applied to a synchronous permanent magnet machine. The effectiveness of the DTC-SVM with the second-order SMC method, incorporating the multivariable filter was substantiated through a comparative analysis utilizing three criteria (ISE, IAE, and ITAE) across various operating modes. The proposed control scheme DTC-SVM-SMC2 is associated with the MVF at a significantly low ripple electromagnetic torque and flux level, due to the extraction of the fundamental component and the more or less sufficient elimination of the continuous component. Fast response robustness, and good accuracy in estimating the torque and flux in the presence of defects, with a good current waveform. It provides better dynamics with decreased torque fluctuations in this fault condition due to the use of MVF. This fault tolerant control aims at achieving and implementing the appropriate strategy so that the system can possibly continue

to operate without endangering the entire system, while maintaining the same degree of dynamic performance and robustness during the fault.




REFERENCES

- [1] T. Orłowska-Kowalska *et al.*, “Fault Diagnosis and Fault-Tolerant Control of PMSM Drives-State of the Art and Future Challenges,” *IEEE Access*, vol. 10, pp. 59979–60024, 2022, doi: 10.1109/ACCESS.2022.3180153.
- [2] S. Kulkarni and A. Thosar, “Direct torque-controlled fault tolerant controller for permanent magnet synchronous motor,” *Journal of Electrical Engineering and Technology (IJEET)*, vol. 12, no. 9, pp. 132–144, 2021, doi: 10.34218/IJEET.12.9.2021.012.
- [3] A. Suti, G. Di Rito, and R. Galatolo, “Fault-tolerant control of a three-phase permanent magnet synchronous motor for lightweight uav propellers via central point drive,” *Actuators*, vol. 10, no. 10, pp. 1–21, 2021, doi: 10.3390/act10100253.
- [4] W. Li, X. Wen, and J. Zhang, “Harmonic current minimization in PMSM drive system using feedforward compensation based on torque ripple estimation,” *2019 22nd International Conference on Electrical Machines and Systems, ICEMS 2019*, pp. 1–5, 2019, doi: 10.1109/ICEMS.2019.8922400.
- [5] H. M. Kim, Y. J. Kim, and S. Y. Jung, “Torque ripple and back EMF harmonic reduction of IPMSM with asymmetrical stator design,” *2017 20th International Conference on Electrical Machines and Systems, ICEMS 2017*, pp. 1–4, 2017, doi: 10.1109/ICEMS.2017.8056477.
- [6] J. Kang, X. Li, Y. Liu, S. Mu, and S. Wang, “Predictive Current Control with Torque Ripple Minimization for PMSM of Electric Vehicles,” *Proceedings - 2018 IEEE International Power Electronics and Application Conference and Exposition, PEAC 2018*, pp. 1–6, 2018, doi: 10.1109/PEAC.2018.8590256.
- [7] T. Nishio, Y. Ryosuke, K. Masahiko, and K. Akatsu, “A Method of Torque Ripple Reduction by Using Harmonic Current Injection in PMSM,” *2019 IEEE 4th International Future Energy Electronics Conference, IFEEEC 2019*, pp. 1–5, 2019, doi: 10.1109/IFEEEC47410.2019.9014937.
- [8] A. Houari, F. Auger, J. C. Olivier, and M. Machmoum, “A new compensation technique for PMSM torque ripple minimization,” *IEEE Industry Application Society-51st Annual Meeting, IAS 2015, Conference Record*, pp. 1–6, 2015, doi: 10.1109/IAS.2015.7356827.
- [9] D. Rekioua and T. Rekioua, “A new approach to direct torque control strategy with minimization torque pulsations in permanent magnets synchronous machines,” *2005 IEEE Russia Power Tech, PowerTech*, pp. 1–6, 2005, doi: 10.1109/PTC.2005.4524699.
- [10] K. He, W. Zhu, and L. Xu, “Research on Torque Ripple Suppression of Permanent Magnet Synchronous Motor,” *IOP Conference Series: Earth and Environmental Science*, vol. 170, no. 4, pp. 1–4, 2018, doi: 10.1088/1755-1315/170/4/042129.
- [11] M. Abdusalam, “Structures and control strategies of parallel and hybrid active filters with experimental validations,” *Ph.D. Thesis*, Department of Electrical Engineering, Université de Lorraine, Metz Cedex, France, 2008.
- [12] A. Boussaid, “Active filtering of harmonics in electrical networks. Contribution to improving electrical energy,” *Ph.D. Thesis*, Department of Electrotechnics-Electronics, Université Frères Mentouri-Constantine, Constantine, Aljazair, 2017.
- [13] G. Tarchala, P. Sobanski, and T. Orłowska-Kowalska, “Fault tolerant sliding mode direct torque control of induction motor with inverter reconfiguration,” *IEEE International Symposium on Industrial Electronics*, pp. 1825–1831, 2017, doi: 10.1109/ISIE.2017.8001526.
- [14] Y. Luo, G. Tan, and C. Su, “Direct Torque Control of Permanent Magnet Synchronous Motor Based on Sliding Mode Variable Structure,” *Open Access Library Journal*, vol. 6, no. 9, pp. 1–10, 2019, doi: 10.4236/oalib.1105758.
- [15] M. H. Salem, Y. Bensalem, and M. N. Abdelkrim, “A Speed Sensor Fault Tolerant Control for a Permanent Magnet Synchronous Motor,” *Proceedings of the 17th International Multi-Conference on Systems, Signals and Devices, SSD 2020*, pp. 290–295, 2020, doi: 10.1109/SSD49366.2020.9364188.
- [16] A. Ammar, A. Bourek, and A. Benakcha, “Implementation of robust SVM-DTC for induction motor drive using second order sliding mode control,” *Proceedings of 2016 8th International Conference on Modelling, Identification and Control, ICMIC 2016*, pp. 338–343, 2017, doi: 10.1109/ICMIC.2016.7804133.
- [17] A. Ammar, A. Bourek, and A. Benakcha, “Robust SVM-direct torque control of induction motor based on sliding mode controller and sliding mode observer,” *Frontiers in Energy*, vol. 14, no. 4, pp. 836–849, 2020, doi: 10.1007/s11708-017-0444-z.
- [18] A. Dahdouh, L. Mazouz, A. Elotri, and B. E. Youcefa, “Multivariable Filter-Based New Harmonic Voltage Identification for a 3-Level UPQC,” *Journal Europeen des Systemes Automatisés*, vol. 56, no. 4, pp. 553–563, 2023, doi: 10.18280/jesa.560405.
- [19] T. S. Ahmed, H. Idir, E. G. Mohamed, and A. Scipioni, “Direct Components Extraction of Voltage in Photovoltaic Active Filter Connected in a Perturbed Electrical Network (Based on Robust PLL Algorithm),” *Energy Procedia*, vol. 74, pp. 966–972, 2015, doi: 10.1016/j.egypro.2015.07.731.
- [20] L. Zhang, S. Wang, and J. Bai, “Fast-super-twisting sliding mode speed loop control of permanent magnet synchronous motor based on SVM-DTC,” *IEICE Electronics Express*, vol. 18, no. 1, pp. 1–6, 2021, doi: 10.1587/ELEX.17.20200375.
- [21] A. Benyamina, S. Moulahoum, H. Houassine, and N. Kabache, “Advanced PLL with multivariable filter and fuzzy logic controller-based shunt active power filter,” *2015 20th International Conference on Methods and Models in Automation and Robotics, MMAR 2015*, pp. 364–369, 2015, doi: 10.1109/MMAR.2015.7283903.
- [22] N. Hamouda, K. E. Hemsas, and H. Benalla, “Comparative study of selective active filtering techniques using Park dq synchronous frame of reference and MVF approach (in France: Etude comparative des techniques de filtrage actif sélectif par référentiel synchrone de Park d-q et approche FMV),” *Mediterranean Journal of Modeling and Simulation (MJMS)*, vol. 1, pp. 89–98, 2014.
- [23] A. Dahdouh, S. Barkat, and A. Chouder, “A Combined Sliding Mode Space Vector Modulation Control of the Shunt Active Power Filter Using Robust Harmonic Extraction Method,” *Algerian Journal of Signals and Systems*, vol. 1, no. 1, pp. 37–46, 2021, doi: 10.51485/ajss.v1i1.17.
- [24] F. Mehedi, R. Taleb, A. B. Djilali, and A. Yahdou, “SMC based DTC-SVM control of five-phase permanent magnet synchronous motor drive,” *Indonesian Journal of Electrical Engineering and Computer Science*, vol. 20, no. 1, pp. 100–108, 2020, doi: 10.11591/ijeecs.v20.i1.pp100-108.




- [25] A. Guezi, A. Bendaikha, and A. Dendouga, "Direct torque control based on second order sliding mode controller for three-level inverter-fed permanent magnet synchronous motor: comparative study," *Electrical Engineering and Electromechanics*, vol. 2022, no. 5, pp. 10–13, 2022, doi: 10.20998/2074-272X.2022.5.02.
- [26] H. Lallouani, B. Saad, and B. Letfi, "DTC-SVM based on Interval Type-2 Fuzzy Logic Controller of Double Stator Induction Machine fed by Six-Phase Inverter," *International Journal of Image, Graphics and Signal Processing*, vol. 11, no. 7, pp. 48–57, 2019, doi: 10.5815/ijigsp.2019.07.04.

BIOGRAPHIES OF AUTHORS



Miloud Bahiddine    is an assistant professor in the Department of Electrical Engineering, University of Mohamed Boudiaf, M'sila, Algeria. He received the Engineer Degree from the University of Badji Mokhtar, Annaba, Algeria and in 2008 and M.S. degrees in Electromechanical Systems Option Electromechanical. His research interests are in electrical drives modeling simulation and control, fault-tolerant control and sliding mode DTC hybrid, fuzzy logic, neural networks, and multi-level voltage inverter modeling and simulation. He can be contacted at email: Miloud.bahiddine@univ-msila.dz.



Ali Belhamra    received the professorship and D.Sc. degree (Doctor Habilitatus) in Electromechanical from University of Badji Mokhtar, Annaba, Algeria. He is a professor of electromechanical in the Graduate Division, Electromechanical Department. He is currently the responsible of the electromechanical Systems Research Laboratory, Department of Electromechanical, Faculty Science of Engineering, University Badji Mokhtar, Annaba, Algeria. Her research interests are in electrical drives modeling simulation and control, control of electromechanical systems, and diagnostic and transport. He can be contacted at email: belhamraali@yahoo.fr.